Acta Pharmacologica Sinica (2016) 37: 1110–1120
www.nature.com/aps

Open

Original Article

Nuclear-targeting TAT-PEG-Asp$_8$-doxorubicin polymeric nanoassembly to overcome drug-resistant colon cancer

Zhen-zhen PAN[1, 2], Hui-yuan WANG[1], Meng ZHANG[1], Ting-ting LIN[1], Wen-yuan ZHANG[1], Peng-fei ZHAO[1], Yi-si TANG[1, 2], Yong XIONG[3], Yuan-er ZENG[2, *], Yong-zhuo HUANG[1, *]

[1]Shanghai Institute of Materia Medica, Chinese Academy of Sciences, Shanghai 201203, China; [2]School of Chinese Materia Medica, Guangzhou University of Chinese Medicine, Guangzhou 510405, China; [3]Shanghai Jiaotong University Affiliated Sixth People's Hospital, Shanghai 200233, China

Aim: Drug efflux-associated multidrug resistance (MDR) is a main obstacle to effective cancer chemotherapy. Large molecule drugs are not the substrates of P-glycoprotein, and can circumvent drug efflux and be retained inside cells. In this article we report a polymer-drug conjugate nanoparticulate system that can overcome MDR based on size-related exclusion effect.
Methods: Doxorubicin was coupled with the triblock polymeric material cell-penetrating TAT-PEG-poly(aspartic acid). The amphiphilic macromolecules (termed TAT-PEG-Asp$_8$-Dox) could self-assemble into nanoparticles (NPs) in water. The antitumor activity was evaluated in drug-resistant human colon cancer HCT8/ADR cells *in vitro* and in nude mice bearing HCT8/ADR tumor.
Results: The self-assembling TAT-PEG-Asp$_8$-Dox NPs were approximately 150 nm with a narrow particle size distribution, which not only increased the cellular uptake efficiency, but also bypassed P-glycoprotein-mediated drug efflux and improved the intracellular drug retention, thus yielding an enhanced efficacy for killing drug-resistant HCT8/ADR colon cancer cells *in vitro*. Importantly, the TAT-PEG-Asp$_8$-Dox NPs enhanced the intranuclear disposition of drugs for grater inhibition of DNA/RNA biosynthesis. In nude mice bearing xenografted HCT8/ADR colon cancers, intravenous or peritumoral injection of TAT-PEG-Asp$_8$-Dox NPs for 22 d effectively inhibited tumor growth.
Conclusion: TAT-PEG-Asp$_8$-Dox NPs can increase cellular drug uptake and intranuclear drug delivery and retain effective drug accumulation inside the cells, thus exhibiting enhanced anticancer activity toward the drug-resistant human colon cancer HCT8/ADR cells.

Keywords: doxorubicin; multidrug resistance; cell-penetrating peptide; poly(aspartic acid); intranuclear delivery; nanoparticles; human colon cancer HCT8/ADR cells

Acta Pharmacologica Sinica (2016) 37: 1110–1120; doi: 10.1038/aps.2016.48; published online 13 Jun 2016

Introduction

Colorectal cancer (CRC) is a serious threat to human health, ranking as the third most commonly diagnosed cancer in males and the second most commonly diagnosed cancer in females, with an estimated 1.4 million new cases and 693 900 deaths occurring in 2012 worldwide[1]. In the clinic, the most common therapy for CRC is surgery combined with chemotherapy[2]. In particular, the use of anticancer drugs in monotherapy or in combined regimens has significantly improved the survival rate in CRC stages III and IV in the past decade[3]. The median survival among patients with metastatic CRC has been extended to >20 months[4]. Despite this progress, the response rate to current systemic therapies is only approximately 50%, and resistance is almost unavoidable in all patients[5].

Multidrug resistance (MDR) is one of the primary obstacles to effective cancer treatment, and ATP transporter-driven drug efflux is the major mechanism responsible for MDR[6]. P-glycoprotein (P-gp), encoded by the MDR1 gene, is the most widely investigated transporter in chemoresistance[7]. P-gp is the main barrier against effective intracellular drug accumulation, which is associated with clinical therapeutic failure in over 90% of patients with metastatic cancer[8, 9]. P-gp inhibitors have been used to overcome MDR in clinical trials, but treatment benefits have been found to be very limited due to

*To whom correspondence should be addressed.
E-mail yzhuang@simm.ac.cn (Yong-zhuo HUANG);
zengyuaner@126.com (Yuan-er ZENG)
Received 2016-01-26 Accepted 2016-03-27

significant side toxicity[10]. Thus, there is a pressing need to develop new approaches that could improve the current chemotherapeutic regimen to overcome MDR.

Nanotechnology is considered a promising strategy to combat cancer multidrug resistance, and nano drugs can be resistant to drug efflux due to the size-exclusion effect and subcellular distribution pattern (*eg*, nucleic-preferential accumulation)[11, 12]. Of note, the efflux subtracts of P-gp is size dependent, limited to small drugs (300–2000 kDa)[13]. The polymeric drug conjugates are also beneficial for anti-MDR therapy due to their increased size. Poly(amino acids) are biodegradable and have been investigated for drug delivery in oncology[14]. For example, several poly(*L*-glutamic acid)-based drug conjugates (*eg*, paclitaxel, cisplatin) are in the advanced development stage.

Here, we developed a novel peptidyl structure-based drug conjugate system for enhanced drug delivery against MDR cancer (Scheme 1). Poly(aspartic acid) was synthesized by solid-phase synthesis and then conjugated to the cell-penetrating TAT peptide-polyethylene glycol (TAT-PEG) through a disulfide bond, thus forming the triblock material TAT-PEG-Asp_8. Doxorubicin (Dox) molecules were further coupled to the Asp_8 segments, and the ASP_8-Dox can self-assemble as a hydrophobic body, whereas the hydrophilic TAT-PEG chains extend outward, forming a nanostructured system (Scheme 2).

Materials and methods

Materials

Fmoc-Asp(OtBu)-OH, 2-chlorotrityl chloride resin, and Fmoc-Cys(OtBu)-OH were purchased from GL Biochem Co, Ltd (Shanghai, China); 1-ethyl-3-(3-dimethylaminopropyl) carbodiimide (EDC), N-hydroxysuccinimide (NHS), N,N-dimethylformamide (DMF), ethyldiisopropylamine (DIEA), 2-(1*H*-benzotriazole-1-yl)-1,1,3,3-tetramethyluronium hexafluorophosphate (HBTU), glutathione (GSH), Verapamil, diethyl ether, 1-hydroxybenzotriazole (HOBt), and triisopropylsilane were purchased from Sinopharm Chemical Reagent Co, Ltd (Shanghai, China); Ellman's reagent, propidium iodide and 4′,6-diamidino-2-phenylindole (DAPI) were purchased from J&K Scientific (Beijing, China); annexin V-FITC was purchased from BioVision Inc (Mountain View, CA, USA). TAT-PEG_{5000}-SH (TAT sequence YGRKKRRQRRR) was synthesized by Qufu Liyang Biochem Co, Ltd (Qufu, China).

Cell lines

The human colon cancer parental cell line HCT8 and the drug-resistant version, HCT8/ADR, were cultured in RPMI-1640 medium supplemented with 10% fetal bovine serum and antibiotics (100 μg/mL streptomycin and 100 U/mL penicillin) at 37 °C in a humidified incubator with 5% CO_2.

Synthesis of Asp_8-Cys and TAT-PEG-Asp_8

Thiolated octo-aspartic acid (Asp_8-Cys) was synthesized using a standard solid-phase synthesis procedure. Asp_8-Cys was then conjugated to TAT-PEG_{5000}-SH via the thiol/disulfide exchange reaction[15]. Briefly, the TAT-PEG_{5000}-SH was dissolved in PBS (pH 8), with the addition of Ellman's reagent. The mixture was stirred for 1 h and was then purified by heparin affinity column to remove excessive Ellman's reagent. The resultant was reacted with Asp_8-Cys to form TAT-PEG-Asp_8 via the disulfide bond. This purified product was confirmed by ^{1}H NMR spectroscopy.

Preparation of TAT-PEG-Asp_8-Dox conjugates

TAT-PEG-Asp_8 and doxorubicin conjugates were prepared based on a carboxyl-to-amine crosslinking method with EDC/NHS. Briefly, NHS and EDC were added to the methanol solution of TAT-PEG-Asp_8 to activate the carboxyl groups of Asp_8. The doxorubicin methanol solution was then added dropwise to the activated TAT-PEG-Asp_8, stirring overnight at room temperature. The polymer-drug conjugates of TAT-PEG-Asp_8-Dox were precipitated by adding excess cool ether. The Dox content in the conjugates was measured by fluorescence spectrophotometry (λex 485 nm and λem 590 nm).

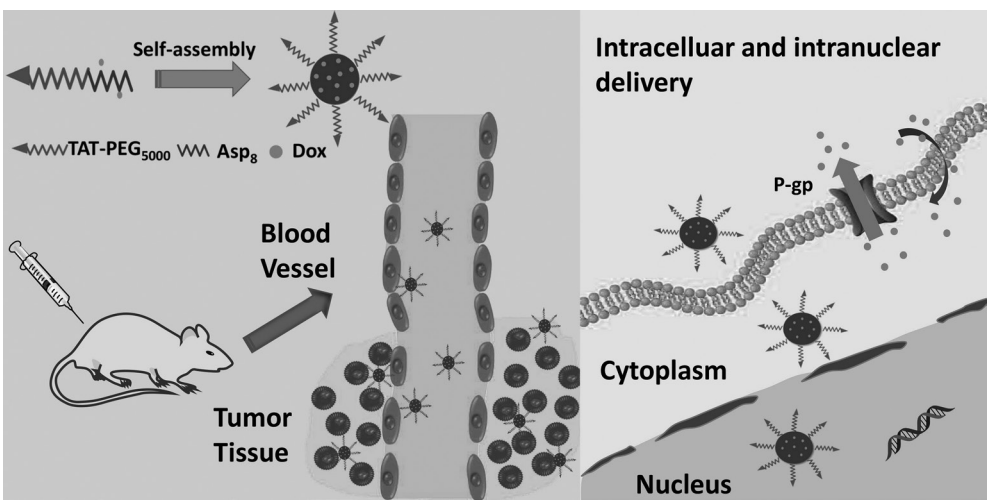

Scheme 1. TAT-PEG-Asp_8-Dox nanoassembly for enhanced drug delivery.

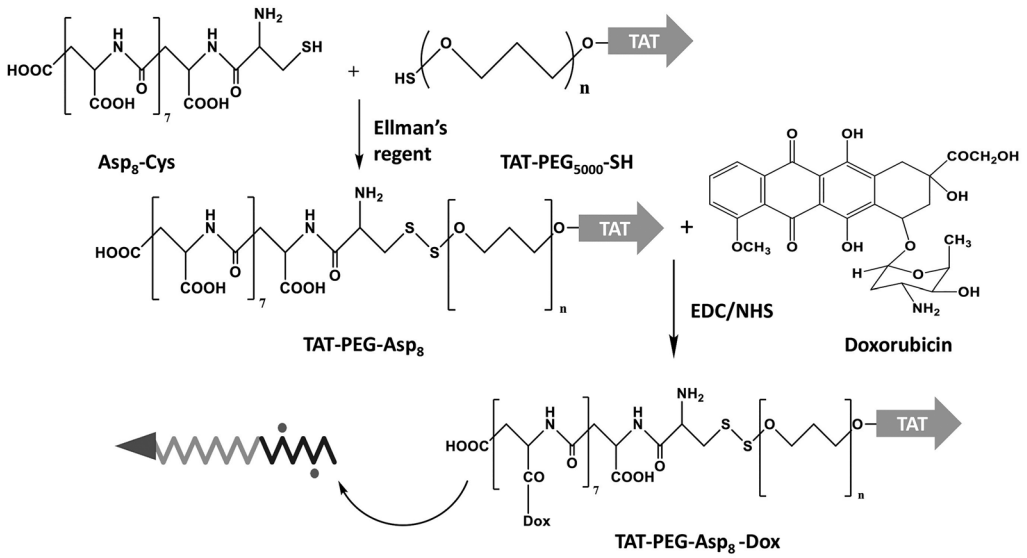

Scheme 2. Synthetic illustration of TAT-PEG-Asp_8-Dox.

Preparation and Characterization of TAT-PEG-Asp_8-Dox NPs

The TAT-PEG-Asp_8-Dox was dissolved in water and self-assembled into nanoparticles. The particle size and zeta potential were measured using a Zeta Sizer Nanoparticle Analyzer (Malvern, UK). The morphology imaging of TAT-PEG-Asp_8-Dox NPs was conducted by JEM-200CX transmission electron microscopy (TEM) with negative staining using uranyl acetate.

Critical micelle concentration and stability of TAT-PEG-Asp_8-Dox nanoparticles (NPs)

The critical micelle concentration (CMC) was determined by fluorescence spectroscopy using pyrene as a hydrophobic fluorescent probe as previously described[16]. Briefly, the sample was prepared at a concentration ranging from 4 to 2×10^{-3} mg/mL and was mixed thoroughly with pyrene solution (2.4×10^{-6} mol/L) at a volume ratio of 1:1. The fluorescence intensity was recorded at Ex 338 nm and 333 nm, and Em 390 nm (F-4600 Fluorescence Spectrophotometer; Hitachi, Japan). The intensity ratio (I_{338}/I_{333}) was plotted against the logarithm of the sample concentration.

The TAT-PEG-Asp_8-Dox NPs were GSH-responsive vehicles due to the disulfide bridge linkage between TAT-PEG and Asp_8. The size change of the NPs treated with GSH (1 μmol/L, 10 mmol/L) at room temperature was measured at different time intervals to evaluate the redox-responsive property of the NPs.

Intracellular and intranuclear delivery of the TAT-PEG-Asp_8-Dox NPs

HCT8 (human colon cancer cell line) and HCT8/ADR (human colon cancer drug-resistant cell line) cells were seeded in 24-well plates at a density of 2×10^4 cells per well and were incubated for 24 h before use.

For cellular internalization observation, the cells were incubated with the TAT-PEG-Asp_8-Dox NPs at an equivalent Dox concentration of 10 μg/mL in fresh culture medium with 10% FBS. After incubation for 4 h, the cellular uptake efficiency was determined by flow cytometry analysis (Becton Dickinson, USA).

For the intranuclear distribution study, after incubation with the TAT-PEG-Asp_8-Dox NPs or free Dox for 4 h, the cells were washed twice with ice-cold PBS and were fixed with fresh 4% paraformaldehyde for 15 min at room temperature. The cell nuclei were counterstained with DAPI, and imaging was performed using confocal laser scanning microscopy (Olympus FV1000, Japan).

Resistance to drug efflux

Intracellular drug retention in the drug-resistant HCT8/ADR tumor cells was investigated by incubation with free Dox or TAT-PEG-Asp_8-Dox NPs for 2 h. After replacement with fresh culture medium supplemented with 10% FBS and further incubation for varying times (0.5, 1, 2, and 4 h), the cells were harvested in 200 μL of DMSO after treatment with RIPA lysis buffer for 10 min. The cell lysate was centrifuged at 8000 rounds per minute, and the supernatant was used to measure the Dox content by fluorescence spectrophotometry.

Effect of verapamil on drug efflux

Verapamil is a commonly used P-gp inhibitor. HCT8/ADR cells were seeded in 24-well plates and were incubated for 24 h before use. The HCT8/ADR cells were pretreated with verapamil (50 μmol/L) for 2 h and then were incubated with free Dox or TAT-PEG-Asp_8-Dox NPs. After incubation for 1 h or 2 h, the cellular Dox intensity was measured by flow cytometry analysis.

In vitro cytotoxicity study

The cytotoxicity of the NPs in the HCT8 and HCT8/ADR cell lines was investigated using the standard MTT assay. Cells were seeded at a density of 5×10^3 cells per well in 96-well plates and were cultured for 24 h before analysis. The cells were incubated with varying concentrations of TAT-PEG-Asp_8-Dox NPs or free Dox for 48 h. MTT (20 μL, 5 mg/mL) was added to each well, and the samples were incubated for another 4 h. After removal of the medium, 200 μL of DMSO was added to each well, and the absorbance was measured at 490 nm using a microplate reader (Multiskan; Thermo Fisher, USA). The cell viability was calculated.

Cell apoptosis assay

The apoptotic cells were detected by flow cytometry. Briefly, the HCT8/ADR cells were seeded in a 6-well plate at a concentration of 2×10^5 cells/well and were cultured for 24 h before analysis. The cells were treated with the TAT-PEG-Asp_8-Dox NPs or Dox at a concentration of 10 μg/mL. After 48 h of treatment, the cells were harvested, washed, and stained with annexin-V/propidium iodide (PI) according to the manufacturer's instructions. The apoptotic cells were measured by flow cytometry analysis (Becton Dickinson, USA).

Western blot assay

P-gp expression in the cells was detected by Western blotting as previously described[17]. Briefly, the cells were lysed, and proteins were separated by SDS-PAGE and were transferred to nitrocellulose membranes using semidry blotting. Primary antibodies, including anti-mouse P-gp (Abcam) and anti-mouse GAPDH (Sigma), were used for Western blotting analysis for overnight incubation at 4 °C.

In vivo cytotoxicity study

The animal study procedures were approved by the IACUC. The studies were conducted on female BALB/c-nu nude mice aged 3–4 weeks. Drug-resistant HCT8/ADR cells were subcutaneously implanted (1×10^6 cells/mouse) on the back. The mice were divided into five groups randomly (six per group): PBS, TAT-PEG-Asp_8-Dox (peritumoral injection, pi), Dox (pi), TAT-PEG-Asp_8-Dox (intravenous injection, iv), Dox (iv). When the tumor reached approximately 100 mm^3, the animals were treated with the NPs equal to a Dox dose of 2 mg/kg per two days over a period of 22 d. The tumor volume and body weight were monitored throughout the study. The tumor volume was calculated using the following formula:

$$V=(L\times W^2)/2$$

At the experimental endpoint, the mice were sacrificed, and the tumors and major organs were harvested and weighed. Histological examination of the major organs was conducted. The organ coefficient was calculated using the following formula:

Organ coefficient (%)=Weight of the organ/Body weight×100%

Tumor penetration

BALB/c-nu nude mice harboring HCT8/ADR breast tumors were treated with Dox or TAT-PEG-Asp8-Dox NPs. After 4 h, the mice were sacrificed, and the tumor tissues were collected for cryosection. The frozen slides were observed using a fluorescence microscope.

Statistics analysis

Data analyses were performed using GraphPad Prism 6. Statistical differences between groups were determined by one-way ANOVA. The Student's *t*-test was used when two parameters were evaluated. The cellular tests were run in triplicate, and animal studies were with six per group. $P<0.05$ was considered significant.

Results

Polymeric drug conjugates have been widely explored. To increase the cell penetration efficiency of such conjugates, cell-penetrating peptide-modified poly(Asp) was synthesized. Cell-penetrating peptides (CPPs) are a class of relatively short peptides that can penetrate the cell membrane and deliver various types of large cargoes (*eg*, proteins, nucleic acids, nanoparticles) into cells[18]. Moreover, the arginine-rich CPP has also been demonstrated to be able to preferentially target the nucleus, where Dox can intercalate with DNA and thus inhibit cell proliferation[19]. Importantly, cell nucleus-targeting delivery has become an emerging method for combating MDR[12, 20].

The synthesized TAT-PEG-Asp_8 was confirmed by ^{1}H NMR (Figure 1A). The self-assembling TAT-PEG-Asp_8-Dox NPs are approximately 150 nm with a narrow particle size distribution (PDI 0.102), indicating good homogeneity (Figure 1B). It is worth noting that NPs with a favorable size (less than 200 nm) could lead to an enhanced permeability and retention (EPR) effect for passive targeting and increase the drug accumulation at tumor sites[21, 22]. TEM was subsequently carried out to investigate the morphology (Figure 1C). Owing to the vacuum working conditions of TEM, the observed size on TEM was smaller than that from dynamic light scattering measurements. The zeta potential was approximately +15 mV (Figure 1D) owing to the modification of cationic TAT. Generally, poly(Asp) NPs have a low efficiency of cell internalization because of their negatively charged nature[23]. TAT was used in this system to improve the intracellular delivery efficiency.

Disulfide bonds were strategically applied to conjugate TAT-PEG to Asp_8. Owing to the highly reducing environment inside tumor cells, the NPs dissembled very quickly. As shown in Figure 2B, the diameter of GSH-treated (10 mmol/L) NPs increased dramatically, reaching approximately 600 nm within 1 h. Further incubation resulted in microsized particles and severe aggregation. However, without GSH treatment (in water) or at a very low GSH concentration, there was merely minor size variation within the same period.

To investigate the cellular internalization, the NPs were incubated with the HCT8 or HCT8/ADR cells for 24 h at an equivalent Dox concentration of 10 μg/mL and were analyzed by flow cytometry. In the non-resistant HCT8 cells, the NPs showed increased intracellular delivery efficiency compared

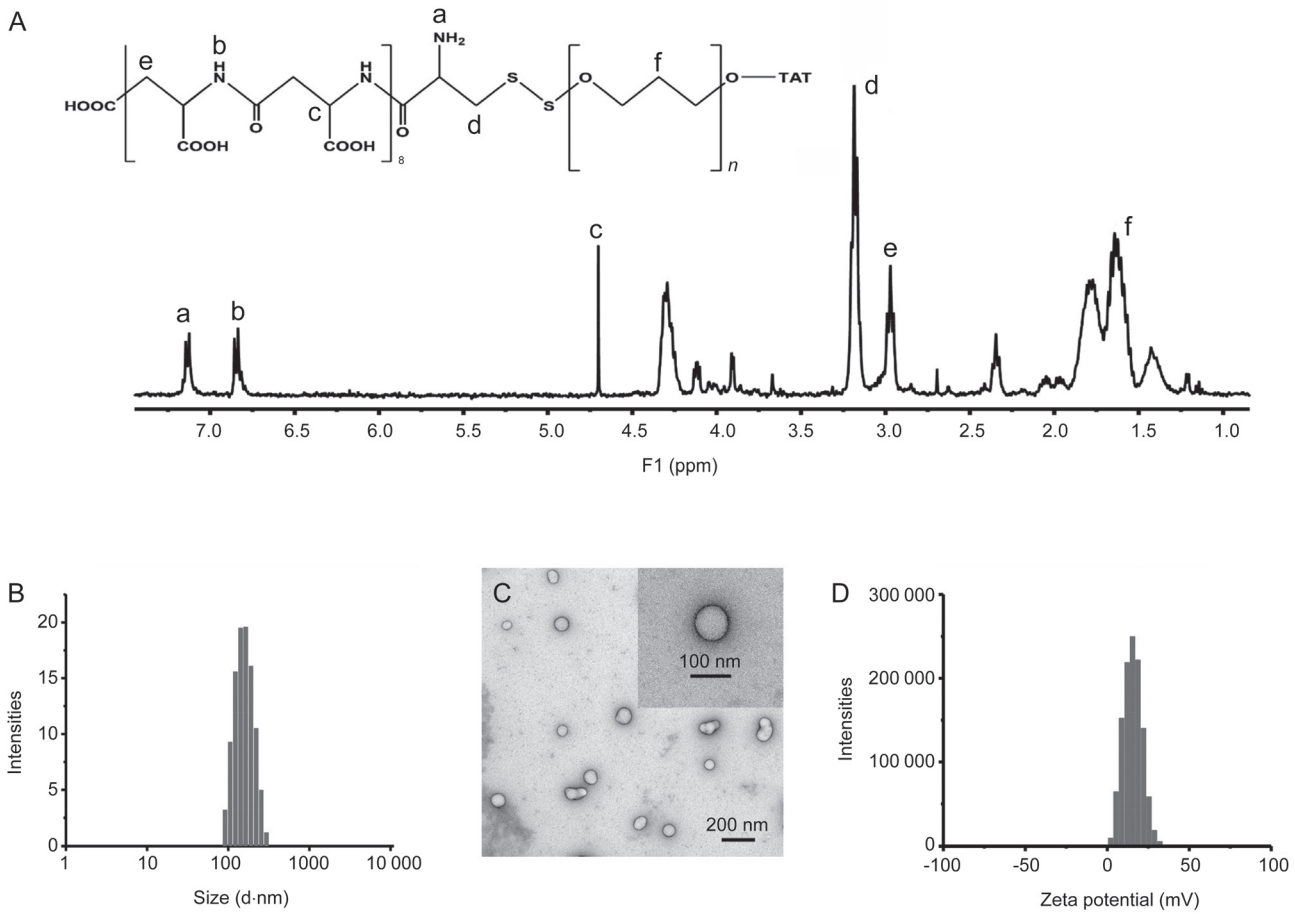

Figure 1. Characterization of TAT-PEG-Asp$_8$. (A) NMR spectrum; (B) size distribution; (C) transmission electron microscopy (TEM); (D) Zeta potential of the nanoparticle (NP).

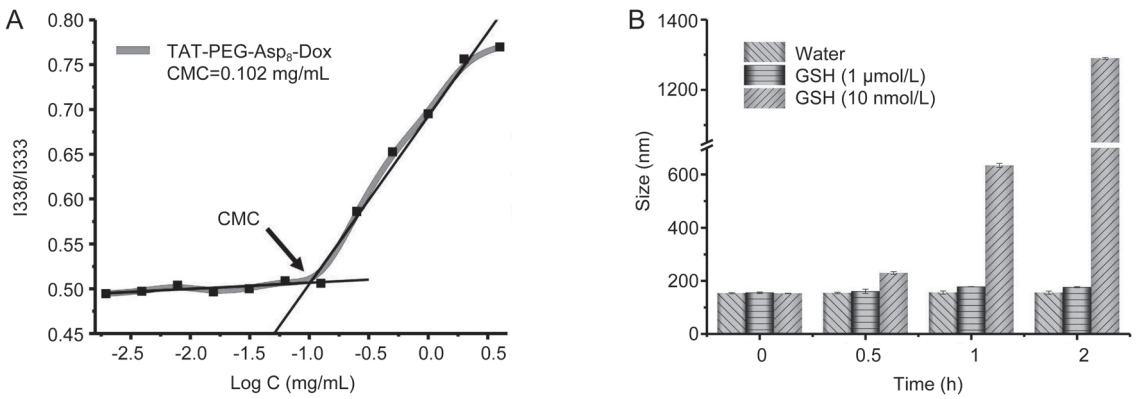

Figure 2. The critical micelle concentration and stability of TAT-PEG-Asp$_8$-Dox. (A) The critical micelle concentration (CMC) of TAT-PEG-Asp$_8$-Dox was about 0.102 mg/mL. (B) NPs size change with or without glutathione (GSH) treatment.

with the free Dox (86.3% *vs* 57.8%, respectively) (Figure 3A). A more significant improvement was seen in the HCT8/ADR cells, which were resistant to drug uptake with a mere 20% positive rate for the free Dox group. However, the NPs were not affected and showed 4.3-fold higher intracellular accumulation than the free Dox. These results demonstrated that the TAT-PEG-Asp$_8$-Dox NPs could overcome drug efflux in HCT8/ADR cells and improve the intracellular accumulation of Dox.

P-gp overexpression in the tumor cell membrane is the

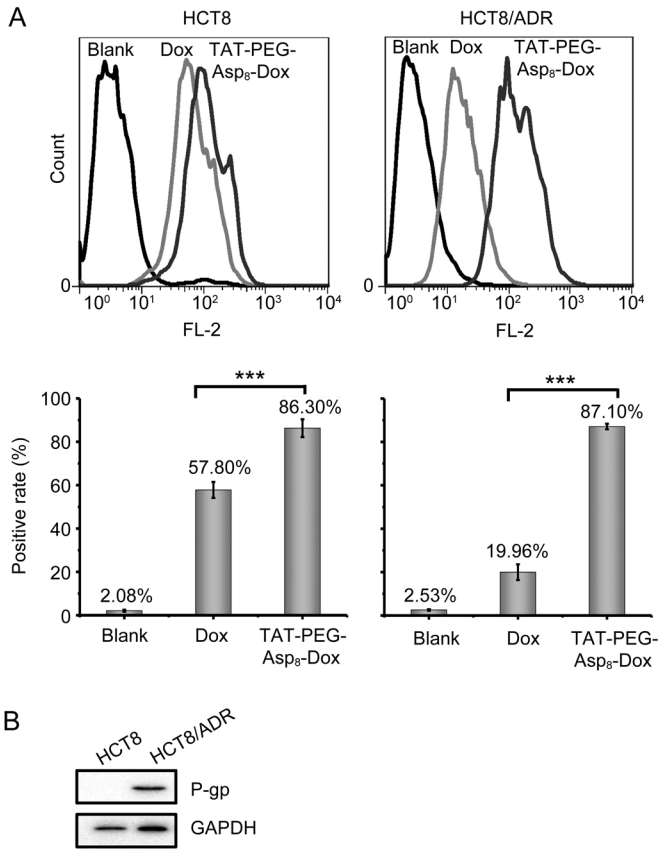

Figure 3. Enhanced intracellular delivery of TAT-PEG-Asp_8-Dox. (A) Uptake efficiency in HCT8 and HCT8/ADR cells ($^{**}P<0.01$); (B) P-gp expression on cells.

major mechanism responsible for MDR. P-gp can actively pump out anticancer drugs, leading to an insufficient intracellular drug concentration to kill tumor cells. Western blot analysis confirmed the high expression of P-gp in HCT8/ADR cells (Figure 3B).

Interestingly, it was found that the NPs could enhance the intranuclear delivery (Figure 4). In the free Dox-treated HCT8/ADR cells, Dox-related red fluorescence was hardly observed due to active drug efflux and consequent poor accumulation. By contrast, intensive red fluorescence was observed in the nuclei in the NP group, indicating the efficient TAT-mediated nuclear localization. The results demonstrated that the TAT-PEG-Asp_8-Dox NPs enhanced not only the cellular uptake but also the intranuclear disposition of drug. The increased intracellular and intranuclear delivery provided a potential solution to overcome MDR in cancer cells, leading to improved therapeutic efficacy.

The intracellular retention results further revealed the advantages of the TAT-PEG-Asp_8-Dox NPs for anti-MDR. The area under the curve (AUC) of the intracellular Dox concentration at 4 h was calculated to be 1183 and 463 $h \cdot ng \cdot mL^{-1}$ for the NP group and free Dox group, respectively (Figure 5). The intracellular drug concentration in the free Dox group was dramatically decreased (merely 45% remaining after 4 h), demonstrating active drug efflux, whereas the NP group was effectively retained inside the cells (76% of the drug remained) because of the resistance to drug efflux.

Verapamil is a commonly used P-gp inhibitor. As shown in Figure 6, there was a clearly increased uptake efficiency in the free Dox group due to the inhibition of drug efflux. However, no significant difference was found in the TAT-PEG-Asp_8-Dox NP group, indicating that TAT-PEG-Asp_8-Dox NPs were not affected by the P-gp-mediated drug efflux.

The cytotoxicity of the TAT-PEG-Asp_8-Dox NPs was investigated in HCT8 and HCT8/ADR cells (Figure 7A). In the HCT8 cells, the NPs displayed slightly better antitumor activity than free Dox, and both of them were potent to inhibit cell proliferation with an IC_{50} of approximately 1 μg/mL. However, the

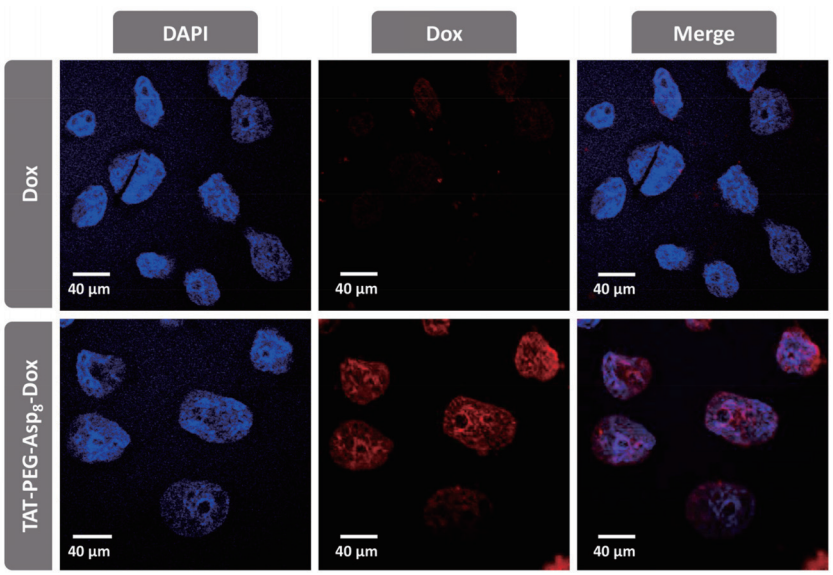

Figure 4. The intranuclear accumulation in HCT8/ADR cells.

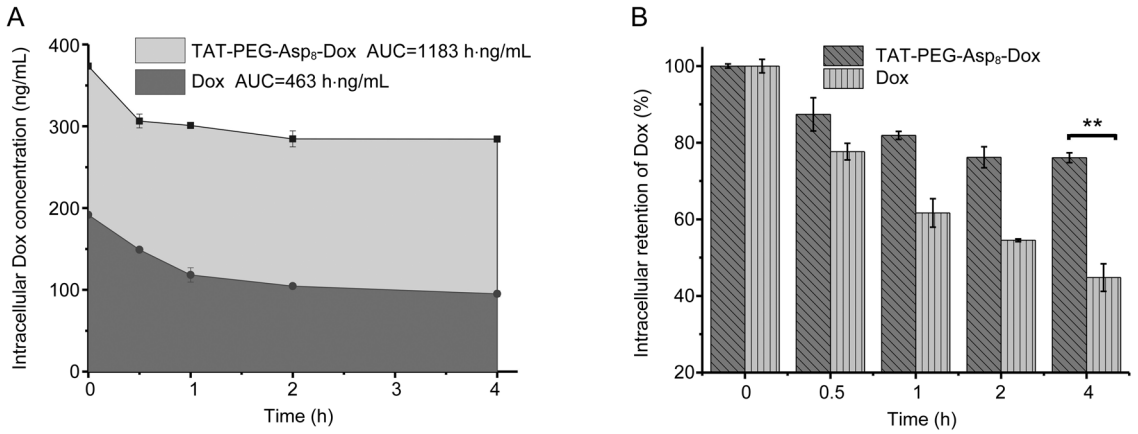

Figure 5. Resistance to drug efflux in HCT8/ADR cells. (A) The area under the curve of intracellular Dox. (B) Intracellular retention of Dox ($^{**}P<0.01$).

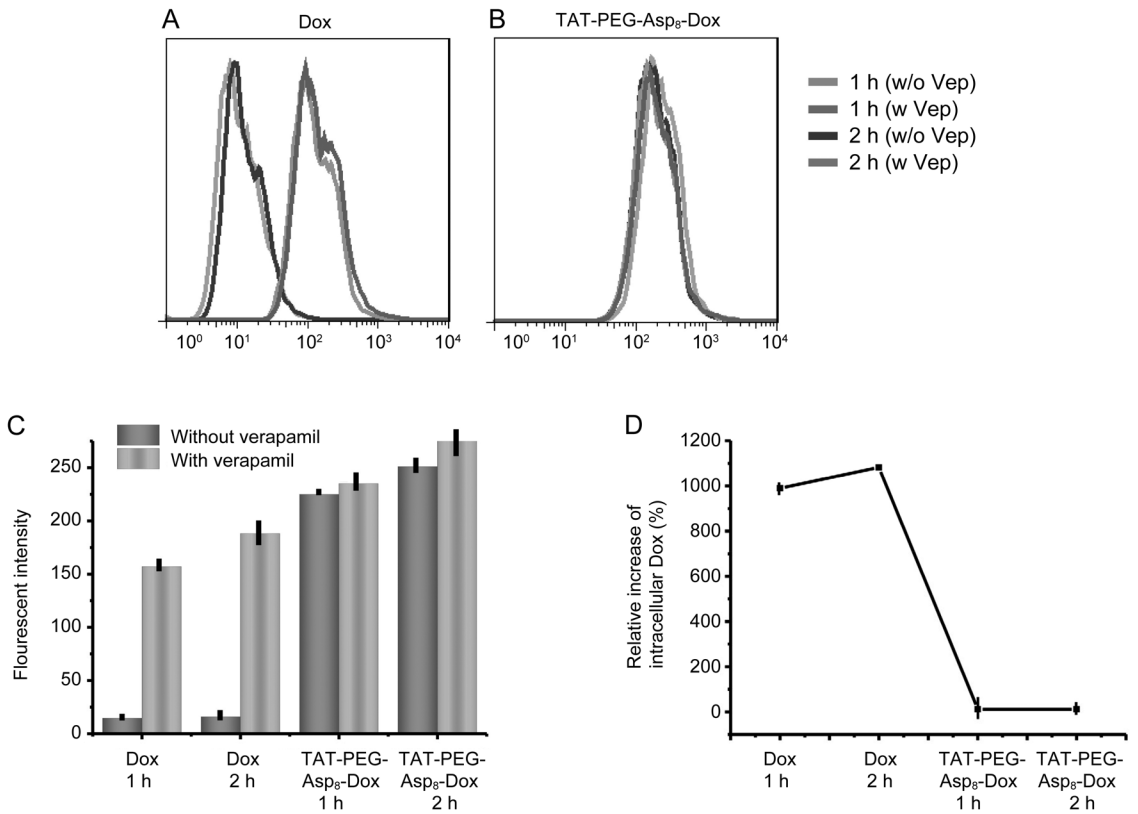

Figure 6. Effect of verapamil in drug-resistant HCT8/ADR cells on intracellular uptake. (A) Verapamil's impact on free Dox. (B) Verapamil had little impact on NPs. (C) Fluorescence intensity in free Dox and TAT-PEG-Asp$_8$-Dox group after verapamil treatment. (D) Relative increase of intracelluar Dox.

NPs still demonstrated high antitumor activity in HCT8/ADR cells, whereas free Dox was ineffective against HCT8/ADR cells even at a concentration up to 20 μg/mL. These results indicated that TAT-PEG-Asp$_8$-Dox NPs could reverse MDR. There are three possible reasons responsible for enhanced cytotoxicity of the TAT-PEG-Asp$_8$-Dox NPs: TAT-mediated enhanced cellular uptake, TAT-mediated intranuclear delivery and enhanced intracellular retention.

Annexin V-FITC and propidium iodide (PI) were used as indicators of early and late apoptosis, respectively. For example, the dual labeling method can indicate intact cells ($FITC^-/PI^-$), cells in early apoptosis ($FITC^+/PI^-$) or late apoptosis ($FITC^+/PI^+$), and necrotic cells ($FITC^-/PI^+$). In HCT8/ADR cells, the late apoptosis rate was determined by flow cytometry, showing 94.6% in the NP group and 38.9% in the free Dox group (Figure 7B), indicating that TAT-PEG-Asp$_8$-Dox NPs could induce apoptosis more efficiently than free Dox in the drug-resistant cells. The results further demonstrated the

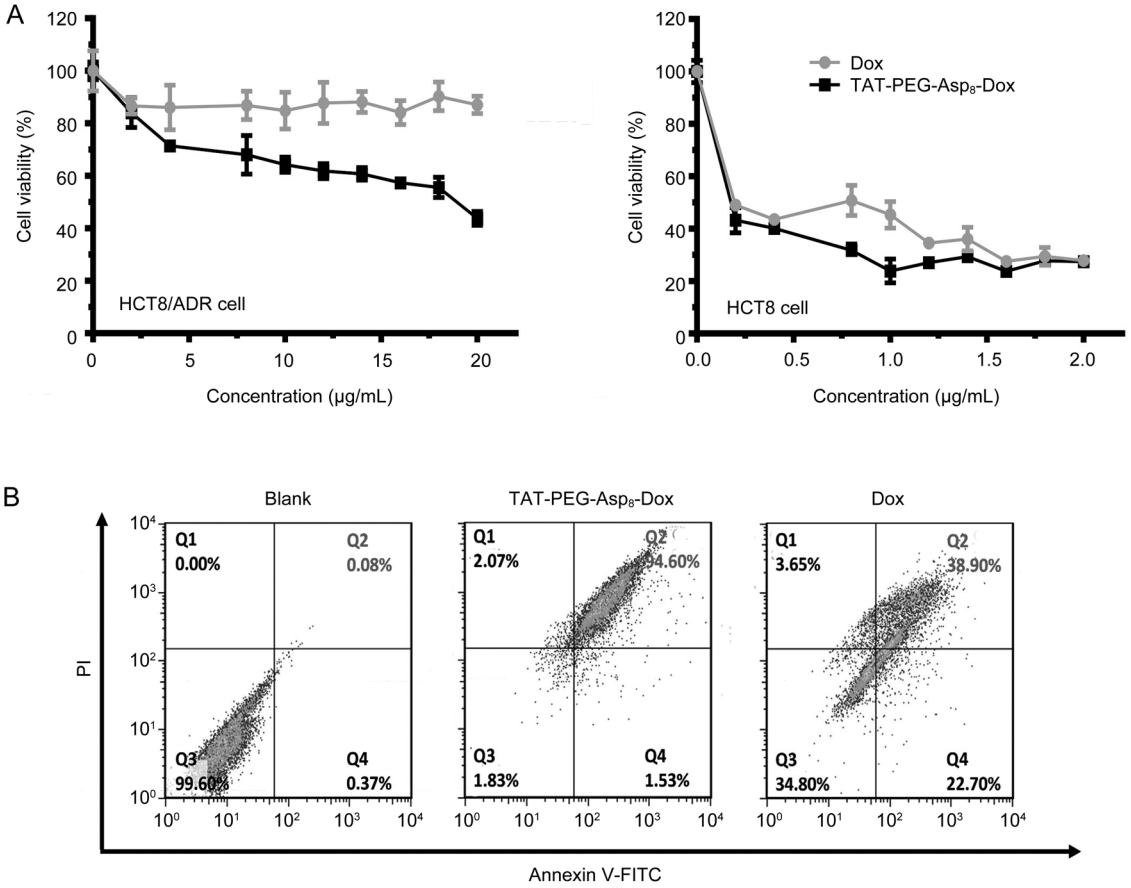

Figure 7. Antitumor activity assay. (A) Cytotoxicity test in HCT8 and HCT8/ADR cell. (B) Cell apoptosis rate.

improved antitumor effect of the TAT-PEG-Asp_8-Dox NPs.

The subcutaneous HCT8/ADR tumor model was employed. The tumor growth curves of each group are presented in Figure 8A. The treatment of the TAT-PEG-Asp_8-Dox NPs resulted in a much smaller tumor volume compared with free Dox therapy. In contrast to an inhibition rate of 71.8% in the iv Dox group, the iv TAT-PEG-Asp_8-Dox NPs exhibited an enhanced efficacy (84.2%), while pi treatment slightly improved the therapeutic efficacy, displaying 89.5% for the TAT-PEG-Asp_8-Dox NPs and 79.1% for free Dox. Therefore, the NPs significantly improved the MDR cancer treatment.

It should be mentioned that the free Dox-treated mice sustained remarkable body weight loss (Figure 9A), and there were two deaths in the iv Dox-treated group (Figure 9B), suggesting the severe side toxicity. However, the animal body weight in the TAT-PEG-Asp_8-Dox NP group underwent minor changes. In addition, at the endpoint, the major organs were collected and weighed to calculate the organ coefficients. In the liver and spleen, the organ coefficient of the iv Dox group was reduced markedly (Figure 9C). Histological examination (Figure 9D) showed degeneration and edema and focal cytolysis necrosis in the liver and spleen in the Dox-treated group. These results indicated that the TAT-PEG-Asp_8-Dox NPs improved the therapeutic efficacy with reduced side toxicity.

In addition, intra-tumoral distribution analysis showed that TAT-PEG-Asp_8-Dox NPs could improve the penetration ability inside tumors compared with free Dox (Figure 10), a finding that was in accordance with our previous studies of CPP-mediated tumor penetration[12].

Discussion

Polymer-drug conjugate strategies have been widely used to improve druggability profiles and therapeutic efficacy. Drug conjugates benefit from increased size when used in MDR cancer therapy to circumvent P-gp-mediated drug efflux. The polymeric drug TAT-PEG-Asp_8-Dox is characterized by its amphiphilic structure: Dox, which is hydrophobic, can form the core, with the peptide-PEG chains, which are hydrophilic, extending from this core, and the drug molecules thereby self-assemble into nanoparticle form.

TAT, which has a similar sequence to a nuclear localization signal (NLS), has demonstrated nuclear-targeting ability[19]. The TAT, which is on the outside of the nanoparticles, can facilitate cellular uptake and intranuclear delivery. Therefore, in addition to the size effect-related resistance to drug efflux, deposit into the nuclei prevents the drugs from being subject

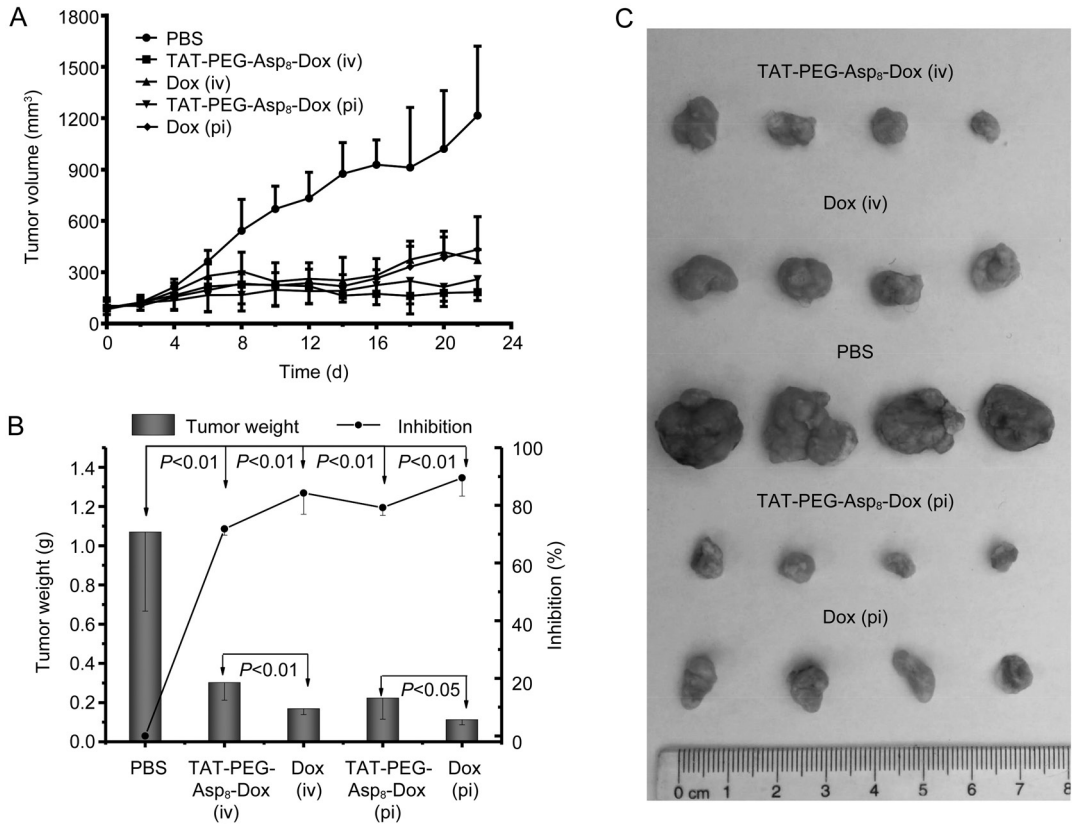

Figure 8. Treatment in nude mice bearing HCT8/ADR tumor. (A) Tumor volume change over the treatment period. (B) Tumor weight at the experimental endpoint and inhibition rate of tumor growth. (C) Representative tumor photos in different groups.

to cell membrane-associated P-gp. Additionally, the CPP-mediated intratumoral penetration could further improve MDR cancer treatment outcomes[12]. Recently, it has been demonstrated that the bio-fate of efficient intratumoral accumulation, penetration, and internalization plays an essential role in cancer drug delivery[24, 25]. TAT-based nano drug delivery provides a useful strategy for enhanced intratumoral drug delivery and treatment.

Concerns regarding nonselective distribution are often raised in CPP-based drug delivery[18]. Recently, however, it has been discovered that CPP can preferentially bind to the tumor cells via certain overexpressed receptors (*eg*, heparan sulfate proteoglycans and neuropilin-1)[26, 27]. We previously also found that CPP-mediated cellular uptake in tumor cells was much higher than that in nontumoral cells (*eg*, human umbilical vein endothelial cells)[12]. These findings suggested that the extravasation of CPP could be minor in normal blood vessels, in contrast to the leaky tumor vessels that are critical to the EPR effect of the nano drugs.

Conclusion

In this study, a TAT-PEG-Asp$_8$-Dox nanoassembly system was developed to sensitize drug-resistant colon cancer to chemotherapy. The TAT-PEG-Asp$_8$-Dox nanoparticles effectively increase cellular drug uptake and intranuclear drug delivery, thus retaining effective drug accumulation inside the cells. The nanoparticles significantly enhanced cytotoxicity toward drug-resistant cells and efficiently induced apoptosis. Therefore, our study reveals a promising method for the efficient intracellular delivery of anticancer drugs and MDR reversal.

Acknowledgements

We are thankful for the support from 973 Program, China (2014CB931900 and 2013CB932503) and National Natural Science Foundation of China (81172996, 81373357, 81422048, 81402883, and 81521005). We also thank National Center for Protein Science Shanghai, CAS, for the technical support at Electron Microscopy Facility.

Author contribution

Zhen-zhen PAN performed most experiments and wrote the manuscript; Hui-yuan WANG participated the cellular and animal studies; Meng ZHANG, Wen-yuan ZHANG, and Ting-ting LIN helped conducted chemical synthesis; Peng-fei ZHAO and Yi-si TANG helped the animal studies; Yong XIONG helped developed the experimental design and reviewed the data; Yuan-er ZENG and Yong-zhuo HUANG designed the study; Yong-zhuo HUANG wrote the final manuscript.

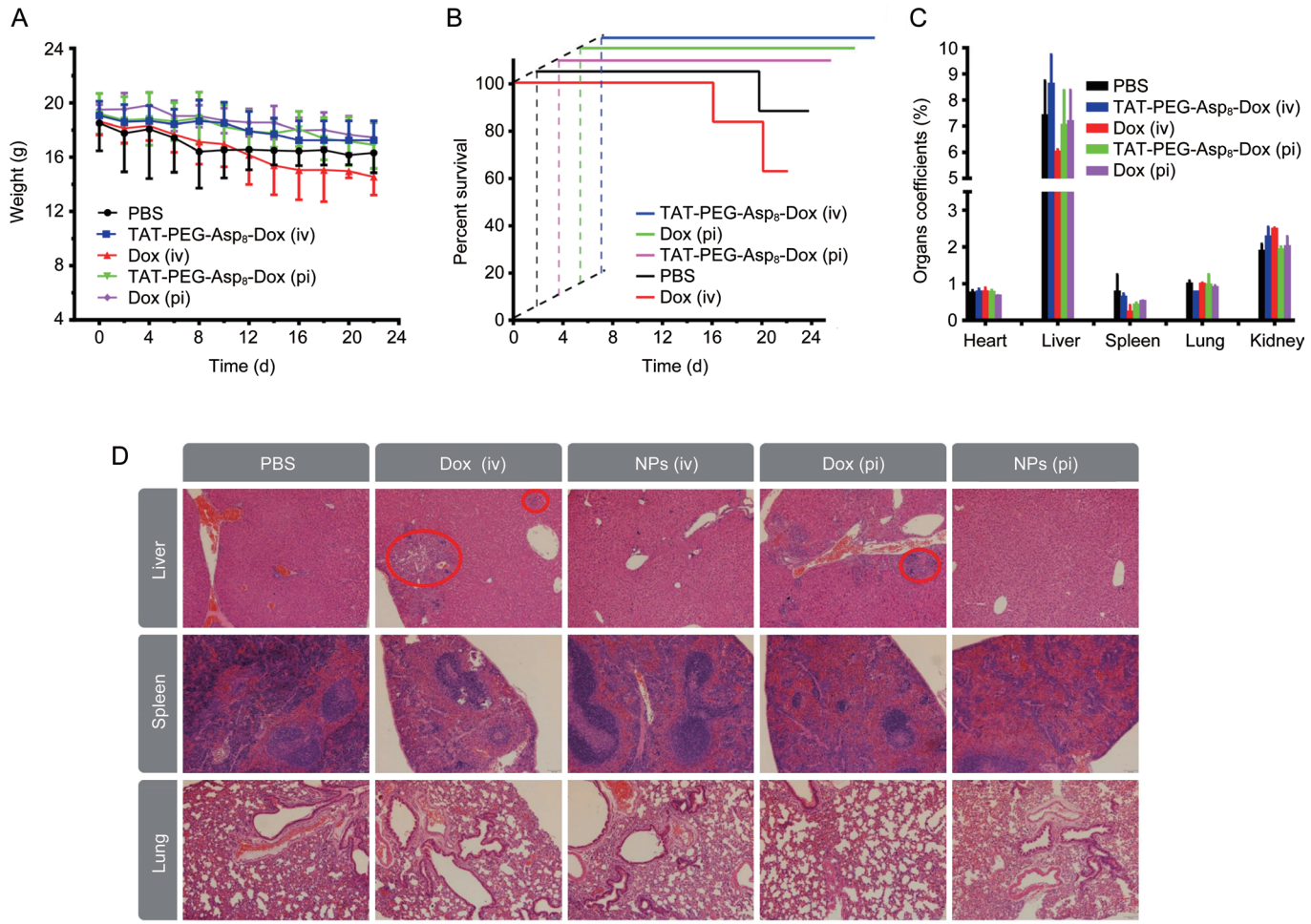

Figure 9. Preliminary evaluation of the treatment safety. (A) body weight change. (B) Survival curves. (C) Organ coefficients. (D) Histopathological examination of major organs after treatment.

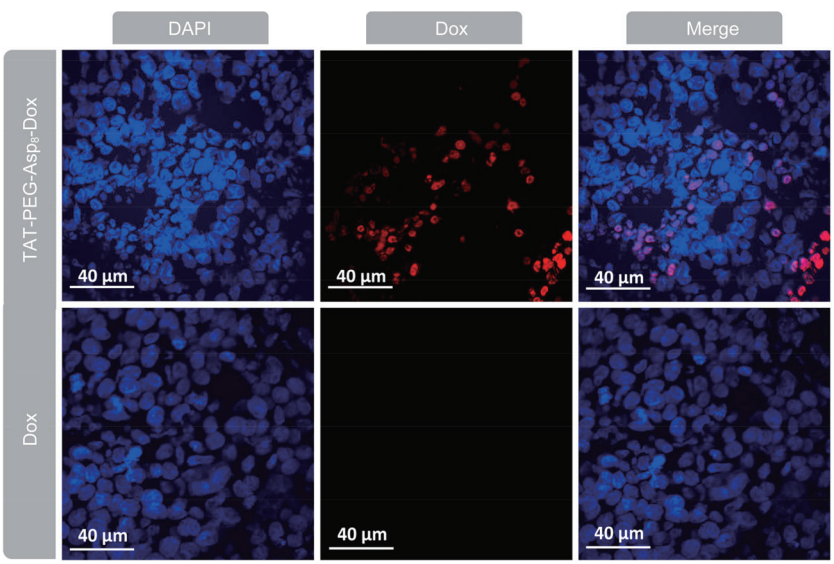

Figure 10. Intratumoral penetration (cryosection slices).

References

1 Torre LA, Bray F, Siegel RL, Ferlay J, Lortet-Tieulent J, Jemal A. Global cancer statistics, 2012. CA: a cancer journal for clinicians 2015; 65: 87–108.
2 Schrag D, Cramer LD, Bach PB, Begg CB. Age and adjuvant chemotherapy use after surgery for stage III colon cancer. Journal of the National Cancer Institute 2001; 93: 850–57.
3 Marin JJ, Sanchez De Medina F, Castano B, Bujanda L, Romero MR, Martinez-Augustin O, *et al.* Chemoprevention, chemotherapy, and chemoresistance in colorectal cancer. Drug Metab Rev 2012; 44: 148–72.
4 Ye LC, Liu TS, Ren L, Wei Y, Zhu DX, Zai SY, *et al.* Randomized controlled trial of cetuximab plus chemotherapy for patients with KRAS wild-type unresectable colorectal liver-limited metastases. J Clin Oncol 2013; 31: 1931–8.
5 Dallas NA, Xia L, Fan F, Gray MJ, Gaur P, Van Buren G, 2nd, *et al.* Chemoresistant colorectal cancer cells, the cancer stem cell phenotype, and increased sensitivity to insulin-like growth factor-I receptor inhibition. Cancer Res 2009; 69: 1951–7.
6 Saraswathy M, Gong S. Different strategies to overcome multidrug resistance in cancer. Biotechnol Adv 2013; 31: 1397–407.
7 Punfa W, Yodkeeree S, Pitchakarn P, Ampasavate C, Limtrakul P. Enhancement of cellular uptake and cytotoxicity of curcumin-loaded PLGA nanoparticles by conjugation with anti-P-glycoprotein in drug resistance cancer cells. Acta Pharmacol Sin 2012; 33: 823–31.
8 Longley D, Johnston P. Molecular mechanisms of drug resistance. J Pathol 2005; 205: 275–92.
9 Shen J, Wang Q, Hu Q, Li Y, Tang G, Chu PK. Restoration of chemosensitivity by multifunctional micelles mediated by P-gp siRNA to reverse MDR. Biomaterials 2014; 35: 8621–34.
10 Callaghan R, Luk F, Bebawy M. Inhibition of the multidrug resistance P-glycoprotein: time for a change of strategy? Drug Metab Dispos 2014; 42: 623–31.
11 Liu J, Zhao Y, Guo Q, Wang Z, Wang H, Yang Y, *et al.* TAT-modified nanosilver for combating multidrug-resistant cancer. Biomaterials 2012; 33: 6155–61.
12 Wang H, Zhao Y, Wang H, Gong J, He H, Shin MC, *et al.* Low-molecular-weight protamine-modified PLGA nanoparticles for overcoming drug-resistant breast cancer. J Control Release 2014; 192C: 47–56.
13 Ueda K, Taguchi Y, Morishima M. How does P-glycoprotein recognize its substrates? Semin Cancer Biol 1997; 8: 151–9.
14 Li C, Wallace S. Polymer-drug conjugates: recent development in clinical oncology. Adv Drug Deliv Rev 2008; 60: 886–98.
15 Hermanson GT. Bioconjugate techniques. Third edition. ed. Academic Press; 2013.
16 Wang H, Li F, Du C, Wang H, Mahato RI, Huang Y. Doxorubicin and lapatinib combination nanomedicine for treating resistant breast cancer. Mol Pharm 2014.
17 Wang H, Wang H, Liang J, Jiang Y, Guo Q, Peng H, *et al.* Cell-penetrating apoptotic peptide/p53 DNA nanocomplex as adjuvant therapy for drug-resistant breast cancer. Mol Pharm 2014; 11: 3352–60.
18 Huang Y, Jiang Y, Wang H, Wang J, Shin MC, Byun Y, *et al.* Curb challenges of the "Trojan Horse" approach: smart strategies in achieving effective yet safe cell-penetrating peptide-based drug delivery. Adv Drug Deliv Rev 2013; 65: 1299–315.
19 Pan L, He Q, Liu J, Chen Y, Ma M, Zhang L, *et al.* Nuclear-targeted drug delivery of TAT peptide-conjugated monodisperse mesoporous silica nanoparticles. J Am Chem Soc 2012; 134: 5722–5.
20 Pan L, Liu J, He Q, Wang L, Shi J. Overcoming multidrug resistance of cancer cells by direct intranuclear drug delivery using TAT-conjugated mesoporous silica nanoparticles. Biomaterials 2013; 34: 2719–30.
21 Davis ME, Shin DM. Nanoparticle therapeutics: an emerging treatment modality for cancer. Nat Rev Drug Disc 2008; 7: 771–82.
22 Peer D, Karp JM, Hong S, Farokhzad OC, Margalit R, Langer R. Nanocarriers as an emerging platform for cancer therapy. Nat Nanotechnol 2007; 2: 751–60.
23 Tran TH, Ramasamy T, Choi JY, Nguyen HT, Pham TT, Jeong JH, *et al.* Tumor-targeting, pH-sensitive nanoparticles for docetaxel delivery to drug-resistant cancer cells. Int J Nanomed 2015; 10: 5249–62.
24 Wang C. Bio-cluster nano-bomb for cancer drug delivery: efficacious fire at the target. Sci Bull 2015; 60: 403–4.
25 Liu X, Xiang J, Zhu D, Jiang L, Zhou Z, Tang J, *et al.* Fusogenic reactive oxygen species triggered charge-reversal vector for effective gene delivery. Adv Mater 2015.
26 Jobin ML, Alves ID. On the importance of electrostatic interactions between cell penetrating peptides and membranes: a pathway toward tumor cell selectivity? Biochimie 2014; 107: 154–9.
27 Kadonosono T, Yamano A, Goto T, Tsubaki T, Niibori M, Kuchimaru T, *et al.* Cell penetrating peptides improve tumor delivery of cargos through neuropilin-1-dependent extravasation. J Control Release 2015; 201: 14–21.